

T. GANCARZ*[#], J. PSTRUŚ***CHARACTERISTICS OF Sn-Zn CAST ALLOYS WITH THE ADDITION OF Ag AND Cu****CHARAKTERYSTYKA ODLANYCH STOPÓW Sn-Zn Z DODATKIEM Ag I Cu**

The aim of this work was to study the effects of Ag and Cu on the thermal properties and microstructure of Sn-Zn-Ag-Cu cast alloys. Solders based on eutectic Sn-Zn containing 0.5 to 1.0 at.% of Ag and Cu were developed for wave soldering. DSC measurements were performed to determine the melting temperatures of the alloys. TMA and electrical resistivity measurements were performed between -50 and 150°C and between 30 and 150°C, respectively. Small precipitates of Cu₅Zn₈, CuZn₄, and AgZn₃ were observed in the microstructures, and their presence was confirmed by XRD measurements. The inclusion of Ag and Cu improved the electrical resistivity and increased the melting temperature, as well as the CTE, of the alloys. However, tests performed to measure the mechanical properties of the alloys demonstrated that the addition of Ag and Cu caused the mechanical properties to decrease.

Keywords: Sn-Zn-Ag-Cu, CTE, electrical resistivity, lead-free solders, XRD, microstructure of cast alloys

Celem pracy było zbadanie wpływu dodatku Ag i Cu na właściwości termiczne i mikrostrukturę stopów Sn-Zn-Ag-Cu. Stopy lutownicze na bazie eutektyki Sn-Zn zawierające od 0,5 do 1,0 % at. Ag oraz Cu zostały opracowane do lutowania falowego. Pomiar DSC wykonywano w celu określenia temperatury topnienia stopów. Badania współczynnika rozszerzalności liniowej przeprowadzono w temperaturach -50 i 150 °C, a oporu elektrycznego od 30 do 150 °C. W mikrostrukturze zaobserwowano drobne wydzielenia Cu₅Zn₈, CuZn₄ i AgZn₃, a ich obecność potwierdzono pomiarami XRD. Dodatek Ag i Cu do eutektyki SnZn obniża rezystywność elektryczną, a podnosi temperaturę topnienia oraz współczynnik rozszerzalności liniowej stopów. Przeprowadzone badania mechaniczne odlanych stopów wykazały, że dodanie Ag oraz Cu spowodowało obniżenie właściwości mechanicznych.

1. Introduction

Sn-Zn eutectic alloy is a replacement for Pb-bearing solder alloys [1], demonstrating better mechanical properties, tensile stress and strain than Sn40Pb and Sn3.5Ag (wt.%) but a lower tensile stress than Sn40Bi (wt.%) [2]. Additionally, this alloy's lower cost per mass unit compared to that of SAC solders meets the low-cost demand of the electronics industry. However, because of the corrosion of Zn [3] and low wear resistance [4], Sn-Zn alloys are often modified with alloying additions, such as Ag [5-7], Al [4, 8, 9], Bi [10], In [11, 12], Ga [13] and Cu [14, 15]. For the Sn9Zn (wt.%) based alloys with Ag additions were found to be suitable for the soldering of Cu and Al [16]. Hung et. al [16] observed precipitates of AgZn₃ on microstructure which has effect on increasing tensile strength and reduce electrical resistivity.

A previous study demonstrated that the addition of a small amount of Al (up to 0.5 wt.%) to eutectic Sn-Zn did not increase its melting temperature [17]. Lin et al. [17] also found that during soldering, the addition of Al reduces the oxygen

content perpendicular to the soldered plane and significantly improves the wettability. Shear strength test results after long-term storage in an 85°C/85% RH environment were high, but they were lower than those for Sn-Pb alloys. The cause of deterioration in the 85°C/85% RH environment is considered to be the deterioration of the Zn constituent at the soldering interface due to the high-temperature vaporization of Zn [17]. The effect of Ag on the oxidation of Sn-Zn alloys was studied by Yeh et al. [18]. The authors found that with an increase in the Ag concentration in the alloy, the layer of oxidized Zn on the alloy's surface is reduced because Ag and Zn form IMCs from the Ag-Zn system.

Das et al. [19] studied the effect of the addition of 0.5 wt.% Al and Cu on the properties of eutectic Sn-Zn alloy, and they found that the effect of this addition on the melting temperature is negligible. The addition of Al to the Sn-Zn alloy caused an increase in the tensile stress but decreased the tensile strain compared with the tensile stress and strain of eutectic Sn-Zn alloy. The effects of the addition of Al, the atmosphere used for processing and temperature on the wettability of

* INSTITUTE OF METALLURGY AND MATERIALS SCIENCE, POLISH ACADEMY OF SCIENCES, 25 REYMONTA STR., 30-059 KRAKOW, POLAND

[#] Corresponding author: t.gancarz@imim.pl

Sn–Zn–xAl alloys were studied by Zhang et al. [20]. The results indicate that with the addition of Al, the wettability of Sn–9Zn solders is improved obviously and for soldering process with flux the optimal addition of Al is about 0.02 (wt %). In soldering at nitrogen atmosphere, the wettability of SnZn–Al on Cu substrate is improved because the surface tension of the Cu substrate increases and the oxidation of the solders decreases, the surface tension of the solders decreases.

The aim of this work was to analyze the effects of the addition of Ag, Al and Cu to Sn–Zn solder on the physical properties and microstructure of cast alloys.

2. Experimental

For the preparation of the alloys, high-purity Sn, Zn, Cu, Al (99.999%) and Ag (99.99%) metals were used. Sn–Zn–Ag–Cu alloys were prepared in a glove box filled with high-purity Ar (99.9999%), with the levels of O₂ and H₂O kept below 1 ppm and the N₂ content kept low, as presented in [11, 21]. The compositions of the studied alloys are reported in Table 1. The melting temperatures of the as-cast alloys were determined by differential scanning calorimetry (DSC) at a heating rate of 10 K min⁻¹. The alloys' microstructures were studied by scanning electron microscopy (SEM) combined with energy dispersive spectroscopy (EDS), whereas their phase compositions were studied by X-ray diffraction (XRD). Linear coefficients of thermal expansion (CTE) were measured using a thermo-mechanical analysis (TMA) tester from -50 to 150°C. The temperature dependence of the electrical resistivity of the alloys were measured from 30 to 150°C using the four-point technique [11]. Mechanical tests were conducted on an INSTRON 6025 testing machine modernized by the Zwick/Roell conditions of testing according to EN ISO 6892-1:2009, with a strain rate of 0.00025 (1/s) at room temperature.

3. Results and discussion

To improve the mechanical and physical properties of the Sn–Zn alloys, Ag and Cu were added [5-7, 14-16], and also a small amount of Al would be added to one of the alloys [17-20] to determine whether its addition would improve the ductility.

Figure 1 presents the results of the DSC analysis of SnZn0.5Ag1.0Cu and SnZn1.0Ag1.0Cu0.1Al alloys. The figure shows a distinct peak close to the melting temperature of eutectic Sn–Zn alloys (199°C) [22]. For the SnZn0.5Ag1.0Cu alloy, a second peak was observed at approximately 280°C, corresponding to liquid alloy with precipitations of AgZn₃,

CuZn₄ and Cu₅Zn₈, which could be expected based on the calorimetric study of ternary Sn–Zn–Ag and Sn–Zn–Cu alloys [23] as well as the recent assessment of the Sn–Zn–Cu system [22]. The same effect involving the appearance of a second peak with the addition of Ag to Sn9Zn0.45Al alloy was observed by Huang [24]; with increasing Ag content, the peak moved to higher temperatures (from 292.4°C for 0.5Ag to 357.7°C for 3.0Ag (wt.%)). For SnZn1.0Ag1.0Cu0.1Al alloy, we observed a peak ending at 327°C. As shown in [23], the peak corresponding to the liquidus transition moves to a higher temperature as a result of increased Ag and Cu contents. Compared with results reported in a study on the effect of the addition of Ag on the melting temperature of eutectic Sn–Zn alloys [24], the present results are shifted toward slightly higher temperatures, which can be associated with the addition of Cu to the alloys.

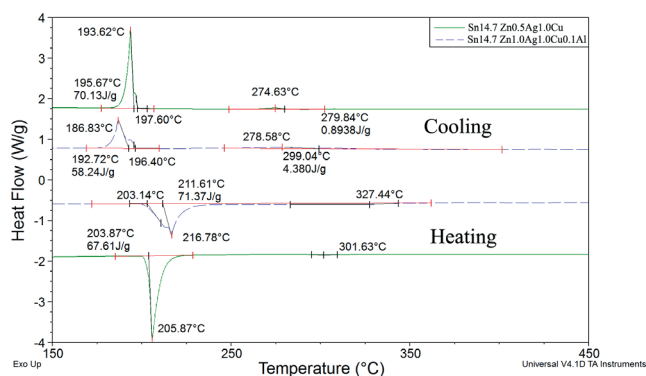


Fig. 1. DSC measurements of Sn14.7Zn0.5Ag1.0Cu (continuous line) and Sn14.7Zn1.0Ag1.0Cu0.1Al (dashed line)

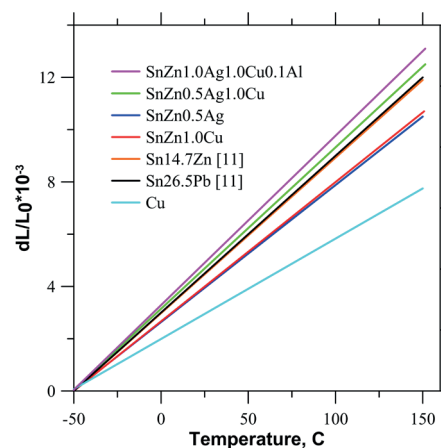


Fig. 2. Linear expansion vs. temperature of Cu, Sn14.7Zn[11], Sn26.5Pb [11], Sn14.7Zn0.5Ag, Sn14.7Zn1.0Cu, Sn14.7Zn0.5Ag1.0Cu and Sn14.7Zn1.0Ag1.0Cu0.1Al

Chemical compositions of the alloys

Alloys	Chemical composition	
	at. %	wt. %
SnZn0.5Ag1.0Cu	Sn14.7Zn0.5Ag1.0Cu	Sn8.7Zn0.5Ag0.6Cu
SnZn1.0Ag1.0Cu0.1Al	Sn14.7Zn1.0Ag1.0Cu0.1Al	Sn8.7Zn1.0Ag0.6Cu0.02Al

TABLE 1

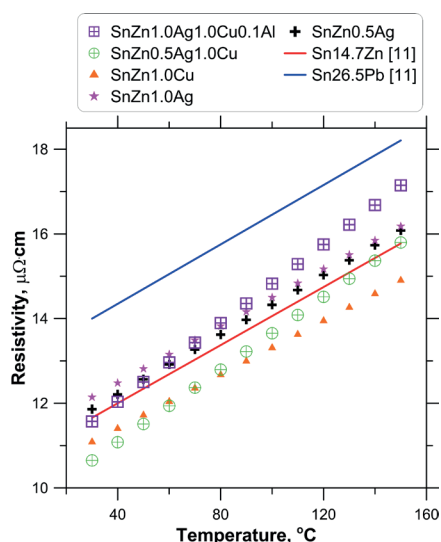


Fig. 3. Electrical resistivity vs. temperature of the following bulk alloys: Sn14.7Zn [11], Sn26.5Pb [11], Sn14.7Zn0.5Ag, Sn14.7Zn1.0Ag, Sn14.7Zn1.0Cu, Sn14.7Zn0.5Ag1.0Cu and Sn14.7Zn1.0Ag1.0Cu0.1Al.

The linear expansion data shown in Fig. 2 for SnZn0.5Ag1.0Cu and SnZn1.0Ag1.0Cu0.1Al alloys are compared with the results of measurements for Cu, eutectic Sn-Zn, eutectic Sn-Pb [11], SnZn1.0Ag, and SnZn1.0Cu (at.%). It can be observed that the obtained CTE parameters (Table 2) for the SnZn0.5Ag1.0Cu and SnZn1.0Ag1.0Cu0.1Al alloys are slightly higher than those of the Sn-Pb [11] eutectic alloy, in contrast to the CTEs of eutectic Sn-Zn [11], SnZn0.5Ag and SnZn1.0Cu alloys, which are lower. As discussed in [11], large differences in the coefficients of thermal expansion (CTEs) between a solder and the corresponding soldered parts may lead to internal tension and result in cracks due to the thermal fatigue of joints. During operation, over variable temperature cycles, the smaller the difference in the CTEs between a solder and a substrate, the less the function of joints will be affected. The results obtained show that with the increase in the amount of additives incorporated into eutectic Sn-Zn, the CTE increases. However, cracks are created in the formation of an intermetallic layer during soldering; therefore, having the CTE of a solder be close to that of the underlying substrate should reduce the formation of cracks.

The electrical resistivity of the following bulk solders are presented in Fig. 3: eutectic Sn-Zn, eutectic Sn-Pb [11], SnZn0.5Ag, SnZn1.0Cu, SnZn0.5Ag1.0Cu and SnZn1.0Ag1.0Cu0.1Al. The addition of Ag to eutectic Sn-Zn gently increases its resistivity, as in the case of eutectic Zn-Al with Ag [21]. At low temperatures, the lowest values of electrical resistivity were obtained for the SnZn0.5Ag1.0Cu alloy, but above 70 $^{\circ}\text{C}$, the lowest electrical resistivity was recorded for the SnZn1.0Cu alloy. Over the studied temperature range, the electrical resistivity of the SnZn1.0Ag1.0Cu0.1 alloy is approximately 10% higher than that of the SnZn0.5Ag1.0Cu alloy but lower than that of eutectic Sn-Pb [11]. The temperature dependence of the quaternary alloys' electrical resistivity has a different slope than that of the ternary or binary alloys, which could be ascribed to the presence of a larger number of IMCs, as observed in the XRD analysis results shown in Fig. 4a and 4b

for the SnZn0.5Ag1.0Cu and SnZn1.0Ag1.0Cu0.1Al alloys, respectively. The Cu_5Zn_8 , CuZn_4 , and AgZn_3 phases were identified by XRD analyses. For the SnZn1.0Ag1.0Cu0.1Al alloy, the dissolution of Al in γ phase Cu_9Al_4 was observed, and the same effect was observed in the study of Sn-Zn-Al [9]

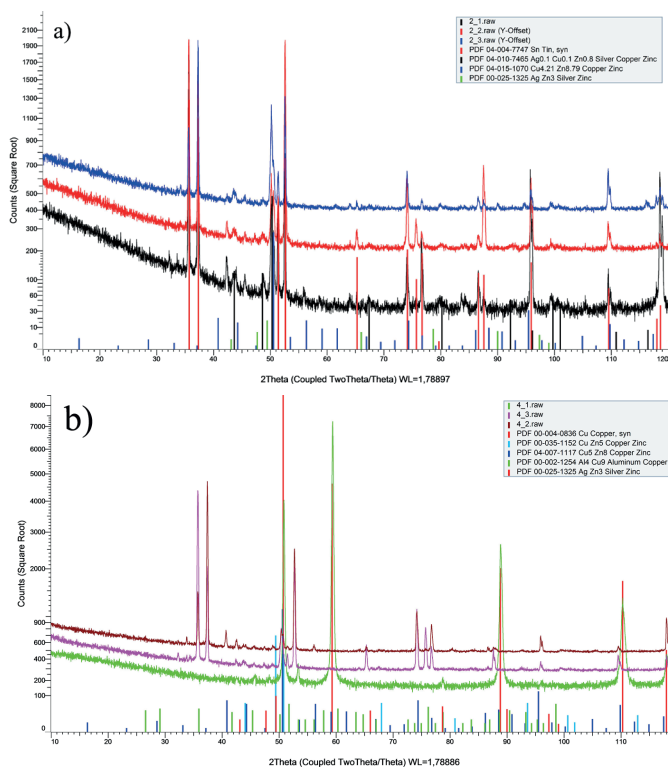


Fig. 4. XRD patterns of the following bulk alloys: a) SnZn0.5Ag1.0Cu and b) SnZn1.0Ag1.0Cu0.1Al

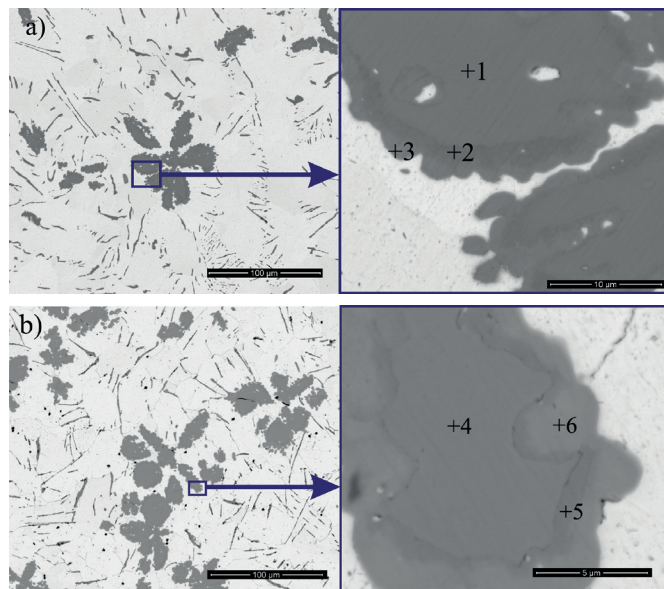


Fig. 5. Microstructures of the following cast alloys: a) SnZn0.5Ag1.0Cu and b) SnZn1.0Ag1.0Cu0.1Al

Fig. 5 presents the microstructures of the SnZn0.5Ag1.0Cu and SnZn1.0Ag1.0Cu0.1Al cast alloys. The microstructures of the cast alloys show precipitates of IMCs. It can be observed that changes appear in the microstructure with the addition of Ag and Al as large areas rich in Ag appear. The results of EDS

analysis at the points indicated in Fig. 5 are shown in Table 3. In the cast alloys with a high Ag content (1%) and 0.1% Al, the SEM and XRD result show a large number of CuZn_4 precipitates surrounded by Cu_5Zn_8 with dissolved Ag as well as small AgZn_3 precipitates. The microstructures of the cast Sn-Zn-Ag-Cu alloys are a combination of the microstructures of the ternary alloys (small AgZn_3 precipitates as in the case of Sn-Zn-Ag alloys [5] and Cu_5Zn_8 precipitates surrounded by CuZn_4 as in the case of Sn-Zn-Cu alloys [15]) against a background structure of a eutectic Sn-Zn matrix. XRD analysis revealed that addition of Ag to eutectic Sn-Zn caused the precipitation of Ag-Zn, as observed by Chen [25]. Furthermore, the small addition of Al dissolved in the $\gamma\text{-Cu}_5\text{Zn}_8$ phase to replace the Zn and convert to Cu_9Al_4 is consistent with the phase diagram of Al-Cu-Zn [26], which is involved in improving the plastic properties of this phase.

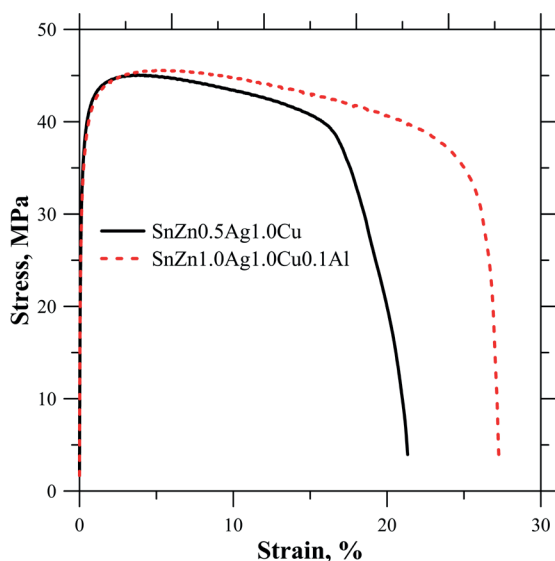


Fig. 6. Tensile stress-strain curves of the SnZn0.5Ag1.0Cu and SnZn1.0Ag1.0Cu0.1Al alloys.

The effect of a third alloying additive on the mechanical properties can be observed in the strain–stress curves shown in Fig. 6. The ultimate tensile strength (UTS) and elongation values are summarized in Table 2. The tensile strengths of the SnZn0.5Ag1.0Cu and SnZn1.0Ag1.0Cu0.1Al alloys were 44.6 and 44.5 MPa, respectively. The elongation of failure values of the SnZn0.5Ag1.0Cu and SnZn1.0Ag1.0Cu0.1Al alloys were 21.4 and 27.4%, respectively. The tensile strength

of 62 MPa obtained by Chen [25] for Sn14.7Zn incorporated with 0.5Ag and Sn14.7Zn is much higher than the values obtained in this study. This discrepancy is attributed to the addition of Cu, which leads to the formation of fragile particles of the Cu_5Zn_8 phase. The high concentration of Ag added, which reached up to 1.0, and the addition of 0.1 Al caused a 6% increase in the elongation of failure, meaning that the addition of Ag did not raise the tensile strength; moreover, the addition of only a small amount of Al improved the plastic properties of the alloys.

TABLE 2

CTE of Sn15Zn0.5Ag1.0Cu and SnZn1.0Ag1.0Cu0.1Al alloys from -50 to 150°C. For comparison, data for Cu, Sn15Zn, Sn26.5Pb, Sn-Zn-Ag, and Sn-Zn-Cu are presented

Alloy at.%	CTE, 10^{-6} K $^{-1}$	Tensile strength (MPa)	Elongation (%)
Cu	15.5	-	-
Sn26.5Pb	24.6 [11]	55 [25]	38 [25]
Sn14.7Zn	20.9 [11]	78 [25]	41 [25]
Sn14.7Zn0.5Ag	21.0	62 [25]	37 [25]
Sn14.7Zn1.0Cu	21.3	-	-
Sn14.7Zn0.5Ag1.0Cu	24.9	44	21
Sn14.7Zn1.0Ag1.0Cu0.1Al	26.2	44	27

4. Conclusions

It was determined that the addition of Ag and Cu increases the melting temperature of Sn-Zn solder, but a peak attributed to the crystallization of Cu-Zn was observed during cooling, as indicated in a new phase diagram of Cu-Sn-Zn [24]. The coefficients of thermal expansion (CTE) increased linearly over the entire temperature range. The CTE for the Sn14.7Zn0.5Ag1.0Cu alloy was higher than the CTEs of the Sn-Zn and Sn-Pb eutectic alloys. In the cast alloys, the microstructure of the eutectic Sn14.7Zn structure with precipitates of AgZn_3 and IMCs from Cu-Zn was observed. The larger precipitates of Cu_5Zn_8 were surrounded by CuZn_4 with dissolved Ag. Increases in the number of precipitates caused a deterioration of the mechanical properties of the alloys. The small amount of Al added dissolved in the $\gamma\text{-Cu}_5\text{Zn}_8$ phase and reduced the fragility of this phase, which improved the plastic properties of the alloy.

TABLE 3

EDS analysis of the cast alloys SnZn0.5Ag1.0Cu and SnZn1.0Ag1.0Cu0.1Al at the points indicated in Fig. 5

	Al	Ag	Cu	Zn	Al	Ag	Cu	Zn
	wt.%				at.%			
1		5.24	29.21	65.55		3.22	30.42	66.36
2		3.4	14.78	81.82		2.08	15.35	82.57
3		13.32	10.95	75.74		8.49	11.84	79.67
4	1.07	4.24	31.34	63.35	2.57	2.55	32	62.88
5		2.91	17.7	79.39		1.77	18.33	79.9
6		14.32	10.08	75.6		9.17	10.96	79.87

Acknowledgments

This work was financed under the framework of the projects POIG.01.01.02-00-015/09 and POIG.02.01.00-12-175/09, which were co-funded by the European Regional Development Fund (ERDF) and the Government of Poland under the Innovative Economy Program.

REFERENCES

- [1] K. Suganuma, *Curr. Opin. Solid. St. M.* **5**, 55-64 (2001).
- [2] W.R. Osório, L.C. Peixoto, L.R. Garcia, N. Mangelinck-Noël, A. Garcia, *J. Alloy Compd.* **572**, 97-106 (2013).
- [3] M.F.M. Nazeri, A.A. Mohamad, *J. Mater. Process. Tech.* (2014), DOI: 10.1016/j.jmatprotec.2014.12.018
- [4] M. Kitajima, T. Shono, *Microelectron. Reliab.* **45**, 1208-1214 (2005).
- [5] K. Berent, P. Fima, J. Pstrus, T. Gancarz, *J. Mater. Eng. Perform.* **23**, 1630-1633 (2014).
- [6] J.-M. Song, P.-C. Liu, C.-L. Snihi, K.-L. Lin, *J. Electron. Mater.* **34**, 1249-1254 (2005).
- [7] J.M. Song, T.S. Lui, G.F. Lan, L.H. Chen, *J. Alloy Compd.* **379**, 233-239 (2004).
- [8] K.L. Lin, H.M. Hsu, *J. Electron. Mater.* **30**, 1068-1072 (2001).
- [9] S.P. Yu, M.C. Wang, M-H. Hon, *J. Mater. Res.* **16**, 76-82 (2001).
- [10] Y.S. Kim, K.S. Kim, C.W. Hwang, K. Sugauma, *J. Alloy Compd.* **352**, 237-245 (2003).
- [11] T. Gancarz, P. Fima, J. Pstrus, *J. Mater. Eng. Perform.* **23**, 1524-1529 (2014).
- [12] M. McCormack, S. Jin, *J. Electron. Mater.* **23**, 715-720 (1994).
- [13] J.M. Song, N.S. Liu, K.L. Lin, *Mater. Trans.* **45**, 776-782 (2004).
- [14] C-Y. Chou, S-W. Chen, *Acta Mater.* **54**, 2393-2400 (2006).
- [15] P. Fima, J. Pstrus, T. Gancarz, *J. Mater. Eng. Perform.* **23**, 1530-1535 (2014).
- [16] M.I. Huang, Y.Z. Huang, H.T. Ma, J. Zhao, *J. Electron. Mater.* **40**, 315-323 (2011).
- [17] K.-L. Lin, L.-H. Wen and T.-P. Liu, *J. Electron. Mater.* **27**, 97-105 (1998).
- [18] T.K. Yeh, K.L. Lin and B. Salam, *Solder. Surf. Mt. Tech.* **21**, 19-23 (2009).
- [19] S.K. Das, A. Sharif, Y.C. Chan, N.B. Wong, W.K.C. Yung, *J. Alloy Compd.* **481**, 167-172 (2009).
- [20] L. Zhang, S.-B. Xue, Li-li Gao, Z. Sheng, H. Ye, Z.-X. Xiao, G. Zeng, Y. Chen, S.-L. Yu, *J. Mater. Sci. Mater. Electron.* **21**, 1 (2010).
- [21] T. Gancarz, J. Pstrus, P. Fima, S. Mosińska, *J. Alloy Compd.* **582**, 313-322 (2014).
- [22] Y-C. Huang, S-W. Chen, C-Y. Chou, W. Gierlotka, *J. Alloy Compd.* **477**, 283-290 (2009).
- [23] J-E. Lee, K-S. Kim, M. Isnoue, J. Jiang, K. Sugauma, *J. Alloy Compd.* **454**, 310-320 (2008).
- [24] C.-W. Hwang, K.-S. Kim and K. Sugauma, *J. Electron. Mater.* **32**, 1249-1256 (2003).
- [25] K-I. Chen, S-Ch. Cheng, S. Wu, K-L. Lin, *J. Alloy Compd.* **416**, 98-105 (2006).
- [26] V. Raghavan, *J. Phase Equilib. Diff.* **28**, 183-188 (2007).

Received: 20 October 2014.

